Check for updates

A MOF-derived ZIF-8@$Zn_{1-x}Ni_xO$ photocatalyst with enhanced photocatalytic activity

Yanqiu Jing,†[a] Jianan Wang,†[a] Baohua Yu,†[b] Jin Lun,[a] Yuyuan Cheng,[c] Bin Xiong,[d] Qiang Lei,[e] Yongfeng Yang,[f] Liangyuan Chen[g] and Mingqin Zhao 🅙 *[a]

Today, metal doped ZnO exhibits good performances and attracts worldwide attention. In this paper, a ZIF-8@$Zn_{1-x}Ni_xO$ photocatalyst was successfully prepared using MOF as precursor and $AgNO_3$ as catalyst. We explored the influence of Ni content on the photocatalytic activity of ZIF-8@$Zn_{1-x}Ni_xO$. The structure and properties of ZIF-8@$Zn_{1-x}Ni_xO$ were characterized by XRD, SEM, FT-IR, BET, UV-vis diffuse reflectance spectroscopy and so on. The results show that Ni is well loaded in ZIF-8 and part of ZIF-8 is oxidized to form $Zn_{1-x}Ni_xO$ composites. The photocatalytic performance of ZIF-8@$Zn_{1-x}Ni_xO$ was evaluated by degradation of rhodamine B (RhB) solution under UV light. It was found that ZIF-8@$Zn_{0.95}Ni_{0.05}O$ exhibited the highest photocatalytic degradation efficiency and can degrade 99.19% rhodamine B solution after 20 min under UV light. Furthermore, ZIF-8@$Zn_{0.95}Ni_{0.05}O$ exhibits high stability. After five repeated cycles, its photocatalytic activity remains at 97.43%.

1. Instruction

Today, organic dyes, such as methylene blue, methyl orange, methyl red, rhodamine B, *etc.*, are widely used in the textile, cosmetic and pharmaceutical industries.[1–3] They play a vital role in our daily life, but they constitute some of the important types of pollutants and can cause permanent injury to humans and animals upon inhalation and ingestion.[4,5] Until now, there have been many ways to solve this problem, such as micro-biological degradation methods, adsorption methods, photocatalytic degradation and so on.[6–8] Among these, the photocatalytic degradation method effective in the remediation of toxic organic pollutants owing to the high mineralization efficiency of semiconductor photocatalysts.[9–13] Until now, lots of semiconductor photocatalysts have been found, such a TiO_2, WO_3, SnO_2, ZnO.[14–17]

ZnO has excellent physicochemical properties, such as for its high chemical stability, non-toxic properties, and excellent photocatalytic activity. It has been widely studied as heterogeneous photocatalyst to degrade organic dyes. With the development of science and technology, it is important to improve its photocatalytic activity. As we know, the photocatalytic activity of ZnO is widely influenced by its band gap and electron–hole pair recombination. So many effects have been made to narrow its band gap and slow its electron–hole pair recombination, such as doping with metals ions,[18] non-metal ions,[19] anchoring with porphyrins and coupling with other semiconductors.[20,21] Furthermore, many researchers have made effects to prepare ZnO composite materials, which possess high specific surface area and have excellent photocatalytic activity.[22]

Zeolitic imidazolate framework-8 (ZIF-8), as a kind of MOFs, has high specific surface area, excellent thermal and chemical stability.[23] It is constructed by Zn(ɪɪ) and 2-methylimidazole ligands and widely used in adsorption, catalytic process and gas separation, *etc.*[24] Bux *et al.* used ZIF-8 membrane to separate ethane from ethane. ZIF-8 membrane exhibits excellent separating property.[25] Zhu *et al.* used ZIF-8 as catalyst to synthesize styrene carbonate from carbon dioxide and styrene oxide. ZIF-8 crystals displayed catalytic activity even at temperatures as low as 50 °C, with styrene carbonate yields as high as ∼54% at 100 °C.[26] Nevertheless, the photocatalytic performance of ZIF-8 is not well applicated.

Ni^{2+}, as a kind of transition metal ions, has been widely used as doping element to prepare Ni doped ZnO, which effectively eliminate the electron hole recombination during photocatalysis.[27,28] In this paper, we firstly used ZIF-8 as precursor and $AgNO_3$ as catalyst to prepare ZIF-8@$Zn_{1-x}Ni_xO$ photocatalyst

[a]College of Tobacco Science, Henan Agricultural University, Zhengzhou, Henan province, China. E-mail: MingqinZhao17@163.com

[b]Economics and Management College, National Tobacco Cultivation and Physiology and Biochemistry Research Centre, Henan Agricultural University, Zhengzhou, Henan province, China

[c]Nanyang Branch of Henan Tobacco Corporation, Nanyang, Henan province, China

[d]Technology Center of China Tobacco Hubei Industrial Co. Ltd., Wuhan, Hubei province, China

[e]Science and Technology Department of Sichuan of China National Tobacco Corporation, Chengdu, Sichuan province, China

[f]Technology Center of China Tobacco Henan Industrial Co. Ltd., Zhengzhou, Henan province, China

[g]Key Laboratory of Tobacco Processing Morphology Research in Tobacco Industry, Zhengzhou, Henan province, China

† Yanqiu Jing, Jianan Wang and Baohua Yu contributed equally to this work and they are all first author.

and explored the influence of Ni content for its photocatalytic efficiency when it used as photocatalyst for degradation of rhodamine B solution. Finally, we systematically analyzed the synergistic effect between ZIF-8 and $Zn_{1-x}Ni_xO$.

2. Experimental

2.1 Chemicals

Zinc nitrate hexahydrate $(Zn(NO_3)_2 \cdot 6H_2O)$, nickel nitrate hexahydrate $(Ni(NO_3)_2 \cdot 6H_2O)$, 2-methylimidazole (2MI), rhodamine B (RhB), silver nitrate $(AgNO_3)$, methanol and ethanol were all analytical reagents and obtained from Sinopharm Chemical Reagent Co. Ltd. All chemicals were directly used without any further purification. Distilled water was used throughout the experiments.

2.2 Preparation of ZIF-8@$Zn_{1-x}Ni_xO$ photocatalyst

The preparation of ZIF-8@$Zn_{1-x}Ni_xO$ includes two procedures. First, we adopted the modified method to synthesize ZIF-8.[29] 40 mmol 2-methylimidazole (2MI) was absolutely dissolved in 100 ml methanol and then slowly poured into another 100 ml methanol containing 10 mmol $Zn(NO_3)_2 \cdot 6H_2O$. The solution was stirred for 5 min and then kept standing at room temperature. After 24 h crystallizing, it was centrifuged and dried at 70 °C to obtain ZIF-8. Second, the synthesized ZIF-8 was used to prepare a series of ZIF-8@$Zn_{1-x}Ni_xO$ photocatalysts containing different of Ni content ($x = 0$, 0.03, 0.05, 0.1). Taking ZIF-8@$Zn_{0.95}Ni_{0.05}O$ for example, 0.95 g ZIF-8 was immersed in the 20 ml ethanol containing 0.05 g $Ni(NO_3)_2 \cdot 6H_2O$ and kept stirring for 60 min. Then, it was directly dried at 70 °C to get the Ni doped ZIF-8 (labelled as ZIF-8@$Ni_{0.05}$). Finally, 1 g ZIF-8@$Ni_{0.05}$ was immersed in 40 ml ethanol solution (38 ml ethanol and 2 ml H_2O) containing 38 mM silver nitrate. After 60 min stirring, it was centrifuged and washed by ethanol for three times to remove the redundant Ag^+ absorbing on the surface and pores of ZIF-8. Subsequently, the sample was dried at 50 °C to obtain the ZIF-8@$Zn_{0.95}Ni_{0.05}O$ photocatalyst. Meanwhile, we used the same procedures to obtain the ZIF-8@ZnO, ZIF-8@$Zn_{0.97}Ni_{0.03}O$, ZIF-8@$Zn_{0.9}Ni_{0.1}O$ photocatalysts. The synthetic procedure of ZIF-8@$Zn_{1-x}Ni_xO$ was shown in Fig. 1.

2.3 Characterization of the products

X-ray powder diffraction (XRD) was carried out to detect the phase of the samples using Bruker-AxsD8 diffractometer with Cu-K_α radiation (operated at 40 kV and 40 mA) in the angular range (2θ) from 5 to 80°. Scanning electron microscopy (SEM) was operated on a Hitachi SU70 microscope to observe the
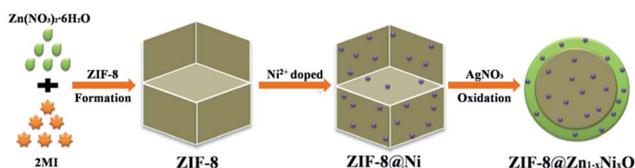
morphology of the samples. The N_2 adsorption–desorption data were obtained from Micromeritics ASAP2020 at −196 °C after degassing the samples at 100 °C for 3 h. The specific surface area of all samples was calculated form the N_2 adsorption–desorption data using Brunauer–Emmett–Teller (BET) equation. UV-vis absorption spectra were determined using a UV-1901 UV-visible spectrophotometer.

2.4 Catalytic activity testing

The photocatalytic activity of all photocatalysts was evaluated by degradation of rhodamine B (RhB) solution under ultraviolet irradiation. The reaction was carried out in a closed box, which contained a 200 ml beaker and a Philips lamp irradiating UV light with the power of 300 W. The distance between the beaker and Philips lamp is 10 cm. In each experiment, 100 ml rhodamine B solution (20 mg L^{-1}), containing 0.1 g ZIF-8@$Zn_{1-x}Ni_xO$, was put into the breaker and stirred continuously in the dark to ensure the adsorption–desorption equilibrium between rhodamine B and ZIF-8@$Zn_{1-x}Ni_xO$. Then, the solution was irradiated under UV light for 20 min. Meanwhile, seven milliliters of the solution was withdrawn from the beaker every five minutes to monitor the residual dye concentration in solution by recording the corresponding changes in the intensity of the absorbance peak at 550 nm as a function of reaction time.

3. Result and discussion

The XRD patterns of all samples are shown in Fig. 2. From Fig. 2, it can be seen that all of the samples exhibit characteristic peaks at 7.38°, 10.42°, 12.77°, 14.75°, 16.50° and 18.08°, which are ascribable to (101), (002), (112), (200), (013) and (222) reflections of ZIF-8.[30,31] When ZIF-8 is treated by $AgNO_3$, it shows new peaks at about 31.77°, 34.42° and 36.25°, which are ascribable to (100), (002) and (101) reflections of ZnO.[32] The doping of Ni do not change the diffraction peaks of ZIF-8@ZnO. It may be the reason that the content of Ni, doped in ZnO, is low.
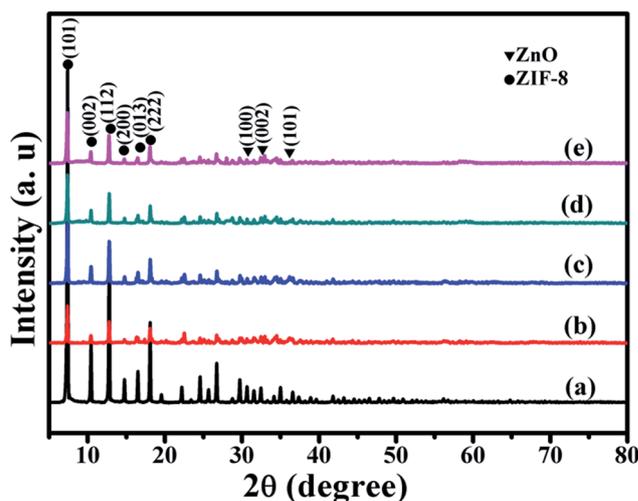

Fig. 1 The synthetic procedure of ZIF-8@$Zn_{1-x}Ni_xO$ photocatalyst.

Fig. 2 XRD patterns of (a) ZIF-8, (b) ZIF-8@ZnO, (c) ZIF-8@$Zn_{0.97}Ni_{0.03}O$, (d) ZIF-8@$Zn_{0.95}Ni_{0.05}O$, (e) ZIF-8@$Zn_{0.9}Ni_{0.1}O$.

From the previous research, we can know that Ag^+ can break coordinative bonds and combine with IM^- to form $HAg(IM)_2$ ($HAg(IM)_2$ represents any silver species coordinated in a linear fashion by IM which also includes polymeric complexes). And Ag^+ can also create a hydroxyl rich environment to transform Zn^{2+} into ZnO. The chemical reactions are proposed to occur as follow:[33]
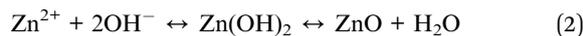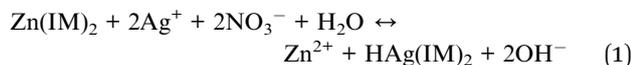
$$Zn(IM)_2 + 2Ag^+ + 2NO_3^- + H_2O \leftrightarrow Zn^{2+} + HAg(IM)_2 + 2OH^- \quad (1)$$

$$Zn^{2+} + 2OH^- \leftrightarrow Zn(OH)_2 \leftrightarrow ZnO + H_2O \quad (2)$$

Fig. 3 shows the SME images of ZIF-8, ZIF-8@ZnO, ZIF-8@Zn$_{0.97}$Ni$_{0.03}$O, ZIF-8@Zn$_{0.95}$Ni$_{0.05}$O and ZIF-8@Zn$_{0.9}$Ni$_{0.1}$O. Fig. 3a is the SEM image of ZIF-8. It can be seen that the synthesized ZIF-8 shows the uniform particle size. Fig. 3b is the high magnification image of ZIF-8. ZIF-8 has cubic morphology. And the particle size of ZIF-8 is about 300 nm. When ZIF-8 is treated by AgNO$_3$, its edges are rounded (Fig. 3c). The morphology of ZIF-8@Zn$_{1-x}$Ni$_x$O, doped with different amount of Ni, shows almost the same.

Fig. 4 is the EDS maps of ZIF-8@Zn$_{0.95}$Ni$_{0.05}$O. It can be seen that ZIF-8@Zn$_{0.95}$Ni$_{0.05}$O exist Zn, O, C, N, Ni elements. The Ni element is well dispersed in ZIF-8@Zn$_{0.95}$Ni$_{0.05}$O nanoparticles. Fig. 4f is the EDS map of Ag in ZIF-8@Zn$_{0.95}$Ni$_{0.05}$O. Ag element is not very clear. It indicates that the content of Ag in ZIF-8@Zn$_{0.95}$Ni$_{0.05}$O is low, which is in agreement with the XRD patterns (Fig. 2) and Wee et al.'s research.[33]

The nitrogen sorption isotherms of ZIF-8@Zn$_{1-x}$Ni$_x$O are shown in Fig. 5. From Fig. 5, it can be seen that ZIF-8@ZnO,
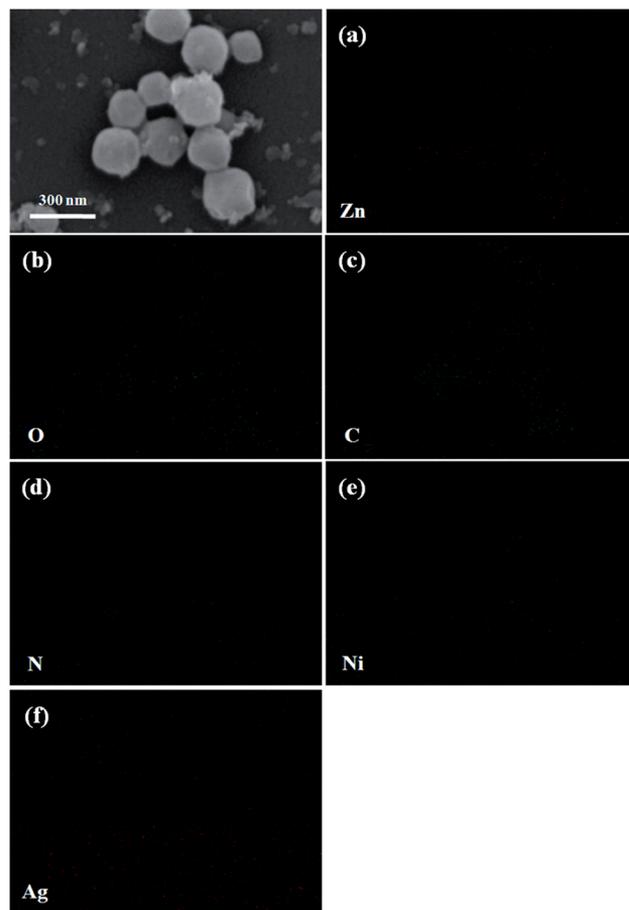

Fig. 4 The EDS maps of ZIF-8@Zn$_{0.95}$Ni$_{0.05}$O.

ZIF-8@Zn$_{0.97}$Ni$_{0.03}$O, ZIF-8@Zn$_{0.95}$Ni$_{0.05}$O and ZIF-8@Zn$_{0.9}$Ni$_{0.1}$O exhibit a type I isotherm pattern and show a significant high uptake in $P/P_0 < 0.1$ region, which is characteristic of microporous materials.[34] When ZIF-8 is oxidized into ZIF-8@ZnO by AgNO$_3$, its microporous volume and BET are 0.32 cm^3 g^{-1} and 803 cm^2 g^{-1},
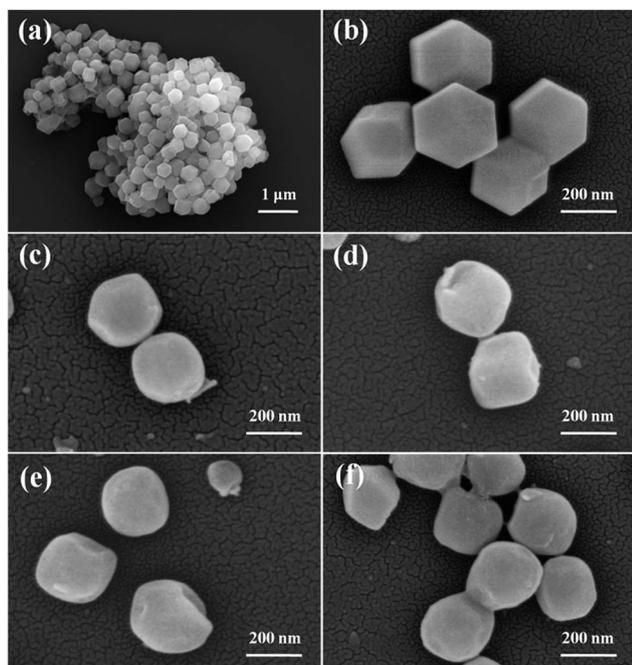

Fig. 3 SEM images of (a and b) ZIF-8, (c) ZIF-8@ZnO, (d) ZIF-8@Zn$_{0.97}$Ni$_{0.03}$O, (e) ZIF-8@Zn$_{0.95}$Ni$_{0.05}$O, (f) ZIF-8@Zn$_{0.9}$Ni$_{0.1}$O.
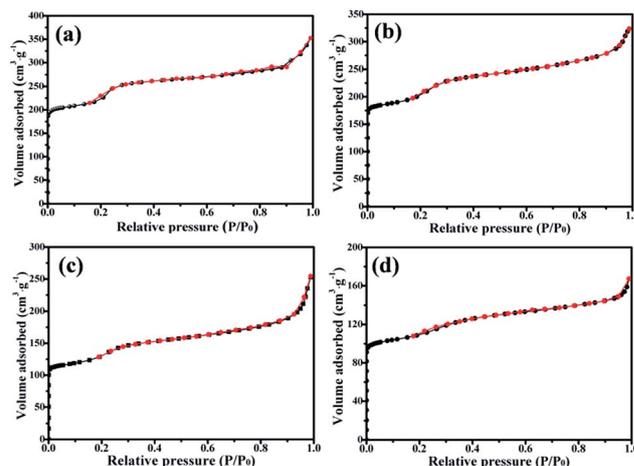

Fig. 5 Nitrogen sorption isotherms of (a) ZIF-8@ZnO, (b) ZIF-8@Zn$_{0.97}$Ni$_{0.03}$O, (c) ZIF-8@Zn$_{0.95}$Ni$_{0.05}$O, (d) ZIF-8@Zn$_{0.9}$Ni$_{0.1}$O.

respectively. When ZIF-8@ZnO is doped with Ni from 3% to 10%, its microporous volume decreases from 0.29 cm^3 g^{-1} to 0.17 cm^3 g^{-1}. And its BET date decreases from 682 cm^2 g^{-1} to 398 cm^2 g^{-1}.

UV-visible absorption spectra of ZIF-8, ZIF-8@Zn$_{0.97}$Ni$_{0.03}$O, ZIF-8@Zn$_{0.95}$Ni$_{0.05}$O andZIF-8@Zn$_{0.9}$Ni$_{0.1}$O are shown in Fig. 6. ZIF-8 shows a strong absorption at about 260 nm. When ZIF-8 is treated by AgNO$_3$, it shows two strong absorptions at 260 nm and 390 nm, which are ascribable to the absorption spectra of ZIF-8 and ZnO, respectively. It indicates that part of ZIF-8 is transformed into ZnO. When ZIF-8@ZnO is doped with 3% Ni, it shows two strong absorptions at 260 nm and 397 nm. The strong absorption of ZnO is shifted to 397 nm. With the increase of Ni content (from 3% to 10%), the absorption spectra of ZIF-8@ZnO increases too (from 390 nm to 425 nm). It indicates that the doping of Ni can decrease the band gap of ZnO.[35]

Rhodamine B was chosen as a model organic dye to evaluate the photocatalytic activity of all photocatalysts. Firstly, every experiment was operated in the dark for 30 min to eliminate the influence of the adsorption of the photocatalyst. The results of RhB adsorption by photocatalysts are shown in Fig. 7a. From Fig. 7a, it can be seen that the after stirring 30 min in the dark, 37.82% RhB is absorbed by ZIF-8. And ZIF-8@ZnO can absorb 32.95% RhB. When ZIF-8 is doped with Ni and oxidized to form ZIF-8@Zn$_{0.97}$Ni$_{0.03}$O, ZIF-8@Zn$_{0.95}$Ni$_{0.05}$O, ZIF-8@Zn$_{0.9}$Ni$_{0.1}$O, its adsorptive property is 30.24%, 28.33%, 24.65%, respectively. The decrease of the adsorptive property of the photocatalysts is attributed to the decrease of its specific surface area. Then, they were exposed under the UV light. The results of RhB degradation by photocatalysts are shown in Fig. 7a. From Fig. 7a, it can be seen that RhB exists self-degradation and can be self-degraded 21.32% after 20 min of UV light irradiation. Meanwhile, the solution, mixture with ZIF-8, just degraded 15.44% of RhB, which is attributed the self-degradation of RhB under UV light. ZIF-8 cannot degrade RhB under UV light. When ZIF-8 is oxidized to form ZIF-8@ZnO, it can degrade 91.25% RhB. When ZIF-8@ZnO is doped with 3%, 5%, 10% Ni, its photocatalytic
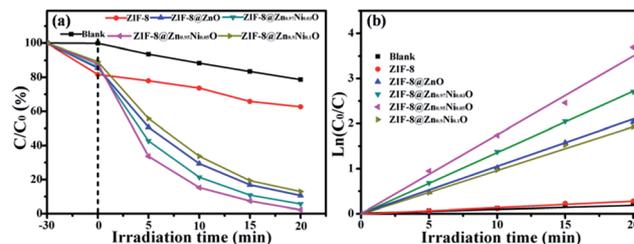

Fig. 7 Photocatalytic degradation (a) and kinetics (b) of photocatalysts for absorption of RhB in the dark and degradation under UV light irradiation.

efficiency is 95.36%, 99.19%, 89.08%, respectively. ZIF-8@Zn$_{0.95}$Ni$_{0.05}$O shows the highest photocatalytic activity. Fig. 7b is the kinetics of photocatalysts for absorption of RhB. The photocatalysis degradation kinetic reaction can be described by $\ln(C_0/C) = kt$ (k is a pseudo-first-rate kinetic constant and t is the irradiation time). The calculated k values of ZIF-8, ZIF-8@ZnO, ZIF-8@Zn$_{0.97}$Ni$_{0.03}$O, ZIF-8@Zn$_{0.95}$Ni$_{0.05}$O and ZIF-8@Zn$_{0.9}$Ni$_{0.1}$O are 0.0145, 0.1085, 0.1375, 0.175 and 0.095 min^{-1}, respectively. ZIF-8@Zn$_{0.95}$Ni$_{0.05}$O shows the highest kinetic constant.

In order to evaluate the separation and reusability of ZIF-8@Zn$_{1-x}$Ni$_x$O, ZIF-8@Zn$_{0.95}$Ni$_{0.05}$O was chosen to degrade RhB solution in five repeated photocatalytic degradation cycles. The results are shown in Fig. 8. From Fig. 8, it can be seen that after five repeated cycles, the photocatalytic activity of ZIF-8@Zn$_{0.95}$Ni$_{0.05}$O is 97.43%. ZIF-8@Zn$_{0.95}$Ni$_{0.05}$O has high separation and reusability. A small decrease in the photocatalytic activity of ZIF-8@Zn$_{0.95}$Ni$_{0.05}$O in the five cycles is possibly due to the inevitable loss of the catalyst during the washing process.[36]

A possible mechanism has been proposed and shown in Fig. 9 to explain the synergistic effects of Ni and ZIF-8 on the photocatalytic activity of ZnO. ZIF-8 has high specific surface area, which can absorb RhB molecules on its surface and pores
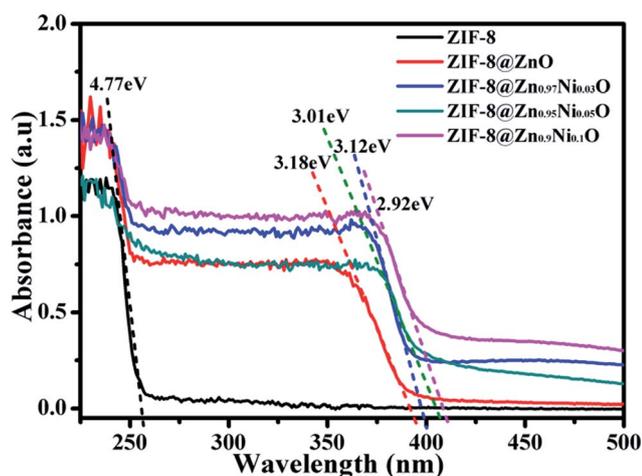

Fig. 6 UV-vis spectra of ZIF-8, ZIF-8@ZnO, ZIF-8@Zn$_{0.97}$Ni$_{0.03}$O, ZIF-8@Zn$_{0.95}$Ni$_{0.05}$O, ZIF-8@Zn$_{0.9}$Ni$_{0.1}$O.
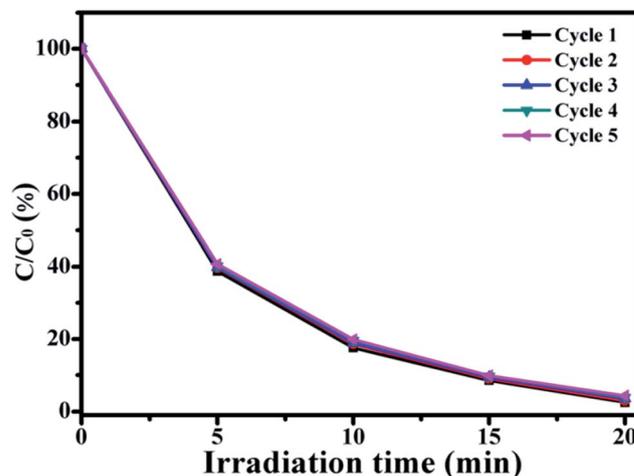

Fig. 8 Five photocatalytic degradation cycles of RhB using ZIF-8@Zn$_{0.95}$Ni$_{0.05}$O under UV light.
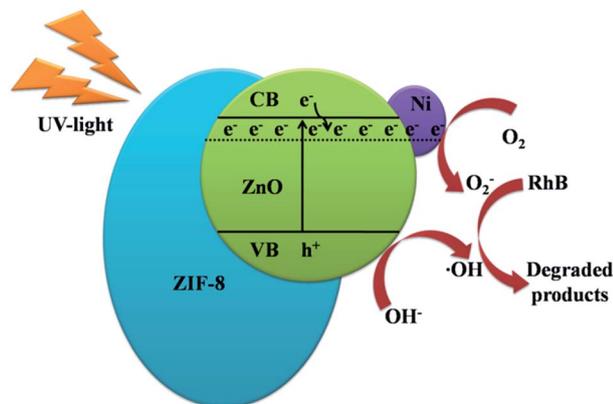
Fig. 9   The schematic illustration of ZIF-8@$Zn_{0.95}Ni_{0.05}O$ for degradation of RhB under UV light.

to form a layer of RhB with high concentration. And the doping of Ni can generate more defects in ZnO. These defects can make the effective separation of electrons and holes, which is irradiated by UV light.[37] The doping of Ni and the incorporation of ZIF-8 make ZnO having high photocatalytic activity.

4.   Conclusions

This paper reports a sample way to synthesize ZIF-8@ZnO and explores the influence of Ni on the structure and properties of ZIF-8@ZnO. The results show that the out surface of ZIF-8 can be transformed into ZnO by using $AgNO_3$ as catalyst. And Ni element has great influence on the photocatalyst activity of ZIF-8@ZnO. When ZIF-8@ZnO is doped with 5% Ni, it shows the highest photocatalyst activity and can degrade 99.19% RhB in 20 min. And ZIF-8@$Zn_{0.95}Ni_{0.05}O$ exhibits high photostability. After five repeated cycles, the photocatalytic activity of ZIF-8@$Zn_{0.95}Ni_{0.05}O$ just reduces by 1.76%. ZIF-8@$Zn_{0.95}Ni_{0.05}O$ has high separation and reusability. The excellent properties of ZIF-8@$Zn_{0.95}Ni_{0.05}O$ make it potential to be used in the treatment of dye pollutants.

Conflicts of interest

There are no conflicts to declare.

Acknowledgements

Notes and references

1 N. O. San, A. Celebioglu, Y. Tümtaş, T. Uyar and T. Tekinay, *RSC Adv.*, 2014, **4**, 32249–32255.

2 T. Kou, C. H. Jin, C. Zhang, J. Z. Sun and Z. H. Zhang, *RSC Adv.*, 2012, **2**, 12636–12643; H. P. Zhao, Y. F. Zhang, G. F. Li, F. Tian, H. Tang and R. Chen, *RSC Adv.*, 2016, **6**, 7772–7779.

3 A. Pal and B. Bag, *RSC Adv.*, 2014, **4**, 10118–11022.

4 S. H. Chen, J. Zhang, C. L. Zhang, Q. Y. Yue, Y. Li and C. Li, *Desalination*, 2010, **252**, 149–156.

5 X. F. Xu, M. Wang, Y. Y. Pei, C. C. Ai and L. J. Yuan, *RSC Adv.*, 2014, **4**, 64747–64755.

6 P. Q. Long, Y. H. Zhang, X. X. Chen and Z. G. Yi, *J. Mater. Chem. A*, 2015, **3**, 4163–4169.

7 M. C. Burtch, H. Jasuja and K. S. Walton, *Chem. Rev.*, 2014, **114**(20), 10575–10612.

8 E. Kowalska, M. Janczarek, L. Rosa, S. Juodkazis and B. Ohtani, *Catal. Today*, 2014, **230**, 131–137.

9 C. L. Yu, Z. Wu, R. Y. Liu, D. D. Dionysiou, K. Yang, C. Y. Wang and H. Liu, *Appl. Catal., B*, 2017, **209**, 1–11.

10 C. L. Yu, W. Q. Zhou, L. H. Zhu, G. Li, K. Yang and R. C. Jin, *Appl. Catal., B*, 2016, **184**, 1–11.

11 X. C. Meng, Z. Z. Li, H. M. Zeng, J. Chen and Z. S. Zhang, *Appl. Catal., B*, 2017, **210**, 160–172.

12 Ş. Ş. Türkyilmaz, N. Güy and M. Özacar, *J. Photochem. Photobiol., A*, 2017, **341**, 39–50.

13 C. L. Yu, L. F. Wei, W. Q. Zhou, D. D. Dionysiou, L. H. Zhu, Q. Shu and H. Liu, *Chemosphere*, 2016, **157**, 250–261.

14 Y. C. Huang, H. B. Li, M. S. Balogun, H. Yang, Y. Tong, X. H. Lu and H. B. Ji, *RSC Adv.*, 2015, **5**, 7729–7733.

15 H. Katsumata, Y. Tachi, T. Suzuki and S. Kaneco, *RSC Adv.*, 2014, **4**, 21405–21409.

16 X. S. Zhu, H. Shi, J. W. Yin, H. M. Zhu, Y. M. Zhou, Y. Tang, P. Wu and T. H. Lu, *RSC Adv.*, 2014, **4**, 34417–34420.

17 R. Saravanan, M. M. Khan, V. K. Gupta, E. Mosquera, F. Gracia, V. Narayanan and A. Stephen, *RSC Adv.*, 2015, **5**, 34645–34651.

18 H. J. Wang, F. Raziq, Y. Qu, C. L. Qin, J. S. Wang and L. Q. Jing, *RSC Adv.*, 2015, **5**, 85061–85064.

19 P. Liang, C. Zhang, H. Q. Sun, S. M. Liu, M. Tadé and S. B. Wang, *RSC Adv.*, 2016, **6**, 95903–95909.

20 Y. Z. Chen, M. B. Yue, Z. H. Huang, L. N. Wang and F. Y. Kang, *RSC Adv.*, 2015, **5**, 23174–23180.

21 M. Y. Nassar, A. A. Ali and A. S. Amin, *RSC Adv.*, 2017, **7**, 30411–30421.

22 Q. Q. Yin, W. J. Wu, R. Qiao, X. X. Ke, Y. Hu and Z. Q. Li, *RSC Adv.*, 2016, **6**, 38653–38661.

23 S. A. Moggach, T. D. Bennett and A. K. Cheetham, *Angew. Chem.*, 2009, **121**, 7221–7223.

24 D. F. Jimenez, S. A. Moggach, M. T. Wharmby, P. A. Wright, S. Parsons and T. Dürent, *J. Am. Chem. Soc.*, 2011, **133**, 8900–8902.

25 H. Bux, C. Chmelik, R. Krishna and J. Caro, *J. Membr. Sci.*, 2011, **369**, 284–289.

26 M. Q. Zhu, D. Srinivas, S. Bhogeswararao, P. Ratnasamy and M. A. Carreon, *Catal. Commun.*, 2013, **32**, 36–40.

27 M. Xiao, Y. F. Lu, Y. G. Li, H. Song, L. P. Zhu and Z. Z. Ye, *RSC Adv.*, 2014, **4**, 34649–34653.

28 J. N. Li, F. Zhao, L. Zhang, M. Y. Zhang, H. F. Jiang, S. Li and J. F. Li, *RSC Adv.*, 2015, **5**, 67610–67616.

29 C. S. Wu, Z. H. Xiong, C. Li and J. M. Zhang, *RSC Adv.*, 2015, **5**, 82127–82137.

30 L. Y. Wang, M. Q. Fang, J. Liu, J. He, L. H. Deng, J. D. Li and J. D. Lei, *RSC Adv.*, 2015, **5**, 50942–50954.

31 J. T. Yoo, S. H. Lee, C. K. Lee, C. R. Kim, T. Fujigaya, H. J. Park, N. Nakashima and J. K. Shim, *RSC Adv.*, 2014, **4**, 49614–49619.

32 X. C. Dong, Y. F. Cao, J. Wang, M. B. C. Park, L. H. Wang, W. Huang and P. Chen, *RSC Adv.*, 2012, **2**, 4364–4369.

33 L. H. Wee, N. Janssens, S. P. Sree, C. Wiktor, E. Gobechiya, R. A. Fischer and C. E. A. Kirschhock, *Nanoscale*, 2014, **6**, 2056–2060.

34 Y. Q. Jing, Y. C. Wang, Y. Z. Gao, H. Q. Li, Y. Y. Cheng, P. Lu, Y. H. Zhang and C. Ma, *RSC Adv.*, 2016, **6**, 42495–42501.

35 Z. Y. Zhang, C. L. Shao, X. H. Li, C. H. Wang, M. Y. Zhang and Y. C. Liu, *ACS Appl. Mater. Interfaces*, 2010, **2**, 2915–2923.

36 S. Senapati, S. K. Srivastava and S. B. Singh, *Nanoscale*, 2012, **4**, 6604–6612.

37 S. M. Mousavi, A. R. Mahjoubm and R. Abazari, *J. Mol. Liq.*, 2017, **242**, 512–519.